Jan CELKO
Martin DECKY
Matus KOVAC

ANALIZA ODDZIAŁYWANIA MIĘDZY POJAZDEM A NAWIERZCHNIĄ DLA CELÓW KLASYFIKACJI IRI W RAMACH SŁOWACKIEGO PMS

AN ANALYSIS OF VEHICLE–ROAD SURFACE INTERACTION FOR CLASSIFICATION OF IRI IN THE FRAME OF SLOVAK PMS

Równość jest jednym z podstawowych czynników jakości nawierzchni. Stanowi ona charakterystykę stanu drogi, jak również bezpieczeństwa na drodze i komfortu jazdy. Nierówności podłużne powodują niedogodności w ruchu drogowym i niebezpieczeństwo zmniejszenia oddziaływania między kołami a nawierzchnią. Wymienione aspekty zostały wzięte pod uwagę w analizie poziomów klasyfikacji w ramach słowackiego PMS. Symulacje różnych warunków brzegowych podczas diagnostyki nawierzchni miały na celu przede wszystkim zbadanie wpływu nierówności na pojazd, a co za tym idzie, na komfort jazdy. Z drugiej strony, wpływ nierówności na oddziaływanie między nawierzchnią a kołem stanowił podstawowe kryterium oceny z punktu widzenia bezpieczeństwa. Przedmiotem artykułu jest obserwacja i ocena opisanych parametrów podczas przeprowadzonych symulacji i pomiarów eksperymentalnych. Do symulacji użyto dynamicznych charakterystyk prawdziwych pojazdów.

Słowa kluczowe: *stan drogi, nawierzchnia, równość, bezpieczeństwo na drodze, niedogodności.*

Road evenness is one from basic factors of the pavement quality. It represents the characteristic of the road serviceability but also road safety and comfortable. The longitudinal unevenness causes the traffic discomfort and danger of the wheel-pavement interaction decreasing. Listed aspects were taken into account for analyze of classification levels in frame of the Slovak PMS. The simulations of different boundary conditions during pavement surface diagnostics were oriented above all to the response of unevenness to the vehicle and to the ride comfort consequently. On the other hand an effect of unevenness to interaction between surface and wheel was the basic criteria of evaluation from safety point of view. The paper is oriented to the observation and evaluation described parameters during realized simulations and experimental measurements. For simulations were used dynamic characteristics of real vehicles.

Keywords: *road serviceability, pavement, evenness, road safety, discomfort.*

1. Introduction

The Slovak Pavement Management System (PMS) [7] is a tool for effective dividing of budget for the management of road rehabilitation. The system includes processes for effective maintenance, repairs and renewal of the road surface and structure. The processes are based on diagnostics of the pavement surface parameters (serviceability level of pavement) and bearing capacity. These parameters input into PMS as follows:

- Surface failures - input by Index of surface deterioration (ISD) describing ratio of failures area to surface area. Evaluation criteria include five levels of quality (from excellent to emergency).
- Longitudinal unevenness - input by International Roughness Index (IRI) describing longitudinal unevenness quality in five levels.
- Transversal unevenness - input by Ruts depth represents the transversal unevenness. The quality is evaluated in five levels scale as for longitudinal unevenness.
- Skid resistance - input by Skid Resistance Index (SRI) describing skid resistance in relation to microtexture and macrotexture quality. The methodology of quality evaluation uses three levels of assessment.
- Bearing capacity uses deflection bowls measured by FWD Kuab as an input for the program CANUV that gives the possibility to determine modulus of pavement layers to calculate residual pavement life and overlay.
- The technology of pavement rehabilitation is chosen according to all the parameters. Evaluation of these variable parameters (except surface failures) in scope of the Slovak PMS and basic principles of PMS are presented in the next part of the paper.

In the next part of the paper are presented correlations of international established dynamic quantifiers of longitudinal unevenness. Following ascertained correlations of parameter C and IRI (International Roughness Index) and new legal regulations has been modified a classification scale of IRI used in Slovakia.

2. International Roughness Index - IRI

Parameter IRI is obtained using the Reference Quarter Car Simulation (RQCS) according to [5] and Fig. 1.

This mathematical model is defined mathematically by two second-order differential equations:

$$\ddot{z}_s \cdot m_s + C_s \cdot (\dot{z}_s - \dot{z}_u) + k_s \cdot (z_s - z_u) = 0 \qquad (1)$$

$$\ddot{z}_s \cdot m_s + m_u \cdot \ddot{z}_u + k_t \cdot z_u = k_t \cdot y \qquad (2)$$

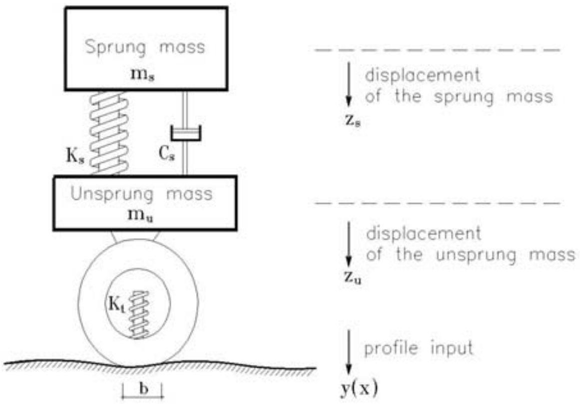

Fig. 1. The Reference Quarter Car Simulation

This system we can express:

$$\ddot{z}_s + C\cdot(\dot{z}_s - \dot{z}_u) + k_2\cdot(z_s - z_u) = 0 \quad (3)$$

$$\ddot{z}_s + u\cdot\ddot{z}_u + k_1\cdot z_u = k_1\cdot y \quad (4)$$

Where: $m_{S,}$ m_U – weight of the sprung mass and the unsprung mass [kg], $k_{S,}$ k_t – constant of the linear spring and the tire [kN.m^{-1}], C_S – coefficient of linear damper [kN.s.m^{-1}], $z_{S,}$ z_U – displacement of the sprung and he unsprung mass [m]

$\dot{z}_s = dz_s/dt$, $\dot{z}_u = dz_u/dt$ - vertical velocity of the sprung/unsprung mass [m.s^{-1}], $\ddot{z}_s = d^2z_s/dt^2$, $\ddot{z}_u = d^2z_u/dt^2$ – vertical acceleration of the sprung/unsprung mass [m.s^{-2}], *y(t)* – profile elevation input [m]

Equations (1) - (4) apply for temporal domain. We solve this model in linear domain, know real longitudinal profile per 0.25 m, whereupon we must find a vector of spatial derivations -$Z^T(x)_{(i)} = (z_{1i}, z_{2i}, z_{3i}, z_{4i})$. The values of this vector are calculated as:

$$z'_{s,i} = s_{11}\cdot z'_{s,i-1} + s_{12}\cdot z''_{s,i-1} + s_{13}\cdot z'_{u,i-1} + s_{14}\cdot z''_{u,i-1} + r_1\cdot y'_i \quad (5)$$

$$z''_{s,i} = s_{21}\cdot z'_{s,i-1} + s_{22}\cdot z''_{s,i-1} + s_{23}\cdot z'_{u,i-1} + s_{24}\cdot z''_{u,i-1} + r_2\cdot y'_i \quad (6)$$

$$z'_{u,i} = s_{31}\cdot z'_{s,i-1} + s_{32}\cdot z''_{s,i-1} + s_{33}\cdot z'_{u,i-1} + s_{34}\cdot z''_{u,i-1} + r_3\cdot y'_i \quad (7)$$

$$z''_{u,i} = s_{41}\cdot z'_{s,i-1} + s_{42}\cdot z''_{s,i-1} + s_{43}\cdot z'_{u,i-1} + s_{44}\cdot z''_{u,i-1} + r_4\cdot y'_i \quad (8)$$

The presented system can be expressed in the following matrix form:

$$Z(x)_{(i)} = \underline{S}\cdot Z(x)_{(i-1)} + R\cdot y'_{(i)} \quad (9)$$

Where: $Z^T(x)_{(i)} = (z_{1,i}; z_{2,i}; z_{3,i}; z_{4,i}) = (z'_{s,i}; z''_{s,i}; z'_{u,i}; z''_{u,i}) = (dz_{s,i}/dx;\ d^2z_{s,i}/dx;\ dz_{u,i}/dx;\ d^2z_{u,i}/dx)$ - vector of spatial derivations, **S** – state transition matrix 4 x 4, **R** – partial response matrix 1 x 4, $y'_{(i)}$ – slope input, *i* – present step, *i*-1 – previous time step.

The differential equations (7) - (10) can be expressed in the following matrix form:

$$Z(t) = \underline{A}\cdot K(t) + B\cdot y(t) \quad (10)$$

Where: $Z^T(t) = (\dot{z}_s, \ddot{z}_s, \dot{z}_u, \ddot{z}_u)$ =(dz$_s$/dt,d^{2}z$_s$/dt,dz$_u$/dt,^{2}z$_u$/dt) -vector of temporal derivations

$K^T(t) = (z_s, \dot{z}_s, z_u, \dot{z}_u)$- additive vector of temporal derivations.

$$\underline{A} = \begin{bmatrix} 0 & 1 & 0 & 0 \\ -K_2 & -C & K_2 & C \\ 0 & 0 & 0 & 1 \\ K_2/u & C/u & -(K_1+K_2)/u & -C/u \end{bmatrix} \quad (11)$$

$$B = \begin{bmatrix} 0 \\ 0 \\ 0 \\ K_1/u \end{bmatrix} \quad (12)$$

For a constant length of the step, on which $y'_{(i)}$ is a constant, the **S** and **R** matrices can be computed from the **A** and **B** matrices:

$$\underline{S} = e^{\underline{A}\cdot dt} \quad (13)$$

$$R = \underline{A}^{-1}\cdot(\underline{S} - \underline{I})\cdot B \quad (14)$$

Where:

dt(s)=dx(m).3600(s/h).0,001(km/m)/ v(kph) (15)

I – identity matrix 4 x 4

The algorithm for evaluation of longitudinal unevenness – IRI KCS, according to original methods [5], has been created in Microsoft Excel 97. This program goes out equations (1)-(15) and one consists of next steps:

Calculation of profile slope input - the profile slope input is computed for every measuring point (we must known elevations of longitudinal profile per 0.25 m):

$$y'_{(i)} = (y_{(i-1)} - y_{(i)})/dx \qquad i = 2,3,.....,N \quad (16)$$

Where: $y'_{(i)}$ – smoothed profile slope input, $y_{(i)}$ - elevation of longitudinal profile [m], *dx* – measurement interval *dx* = *b* = 0,25 m.

Computation of the vector of spatial derivations Z(x)$_{(i)}$ - the computation of vector $Z^T(x)_{(i)} = (z_{1,i}; z_{2,i}; z_{3,i}; z_{4,i}) = (z'_{s,i}; z''_{s,i}; z'_{u,i}; z''_{u,i})$ is realised by equation (15):

$$Z(x)_{(i)} = \underline{S}\cdot Z(x)_{(i-1)} + R\cdot y'_{(i)}$$

Where:

S – state transition matrix 4 x 4, **R** – partial response matrix 1 x 4, *i* – present step, *i*-1 – previous time step

Determination of the corrected profile slope

$$T_i = (z_{3i} - z_{1i}) \qquad i=2,3,...,N \quad (17)$$

Calculation of the parameter IRI - IRI represents arithmetic average of the corrected slope. Values of parameter IRI can be appreciated for window of a discretionary length (conveniently 1, 10, 20, 100 m – Fig.2 right).

$$IRI = \frac{1}{N-1}\cdot\sum_{i=2}^{N} T_i \quad (18)$$

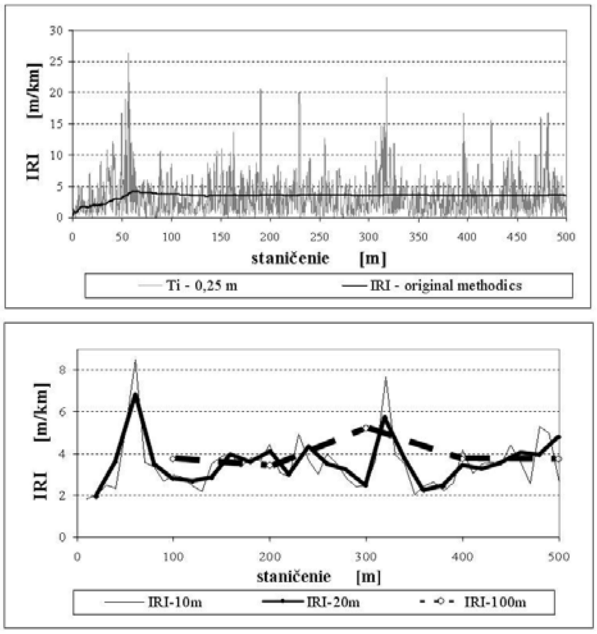

Fig. 2. Corrected profile slope per 0,25 m and original parameter IRI (left) and IRI appreciated for window 10, 20 and 100 m (right)

3. Verification of RQCS model

The measuring set called the Single-Wheel Vehicle of the University of Žilina (Slovak abbr. JP VŠDS) was designed on the DMS (double-mass measuring set) principle. This equipment represents a model of a quarter of the passenger vehicle and its basic parts are presented in Fig.3. The equations of motion for dynamic model JP VŠDS according to Fig. 3 are as follows:

$$m_1\ddot{x}_1 = k_1\left(x_0 - x_1\right) - f_{21} \quad (19)$$

$$m_2\ddot{x}_2 = f_{12} \quad (20)$$

In the case of small vibrations (ϕ_1, ϕ_2 < 5°) the vertical displacements are given by relations $x_1 = l_1\phi_1$ and $x_2 = l_2\phi_2$. The force f_{21} in Eq. 19 means the force effect of suspension spring and damper onto the mass m_1 in the direct of its vertical axle. On the base of moment equation to the cardan joint, the force f_{21} could be expressed as follows:

$$\begin{aligned} f_{21} &= k_2\frac{a^2}{l_1}\left(\varphi_1 - \varphi_2\right) + b_2\frac{a^2}{l_1}\left(\dot{\varphi}_1 - \dot{\varphi}_2\right) = \\ &= k_2\frac{a^2}{l_1^2}x_1 - k_2\frac{a^2}{l_1 l_2}x_2 + b_2\frac{a^2}{l_1^2}\dot{x}_1 - b_2\frac{a^2}{l_1 l_2}\dot{x}_2 \end{aligned} \quad (21)$$

Similar, the force f_{12} in Eq. 20 presents the force reduction effect on the mass m_2 in direct of its vertical axle:

$$\begin{aligned} f_{12} &= k_2\frac{a^2}{l_2}\left(\varphi_1 - \varphi_2\right) + b_2\frac{a^2}{l_2}\left(\dot{\varphi}_1 - \dot{\varphi}_2\right) = \\ &= k_2\frac{a^2}{l_1 l_2}x_1 - k_2\frac{a^2}{l_2^2}x_2 + b_2\frac{a^2}{l_1 l_2}\dot{x}_1 - b_2\frac{a^2}{l_2^2}\dot{x}_2 \end{aligned} \quad (22)$$

The equations of motion for small vibrations are given after substituting the Eqs. 21, 22 into Eqs. 19,20 by:

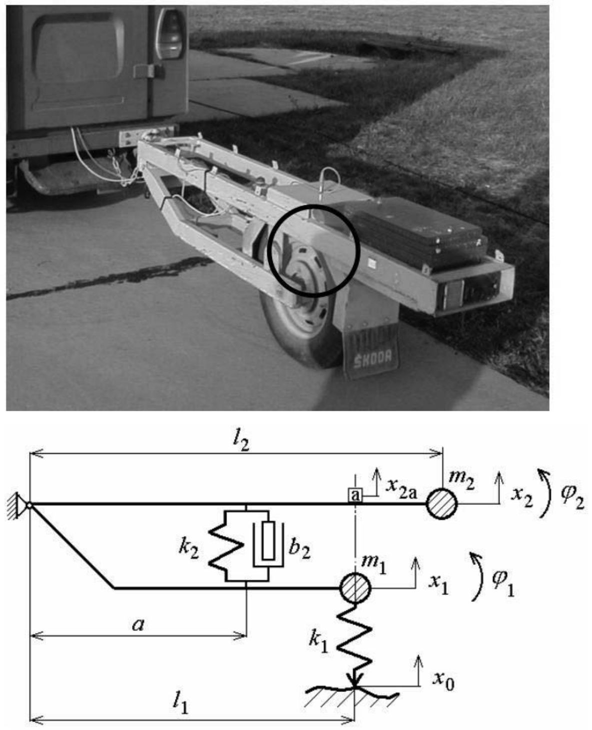

Fig. 3. Single-Wheel Vehicle of the University of Žilina

$$m_1\ddot{x}_1 + b_2\frac{a^2}{l_1^2}\dot{x}_1 - b_2\frac{a^2}{l_1 l_2}\dot{x}_2 + \left(k_1 + k_2\frac{a^2}{l_1^2}\right)x_1 - k_2\frac{a^2}{l_1 l_2}x_2 = k_1 x_0 \quad (23)$$

$$m_2\ddot{x}_2 + b_2\frac{a^2}{l_2^2}\dot{x}_2 - b_2\frac{a^2}{l_1 l_2}\dot{x}_1 + k_2\frac{a^2}{l_2^2}x_2 - k_2\frac{a^2}{l_1 l_2}x_1 = 0 \quad (24)$$

In fact, we do not measure acceleration on the mass m_2 but on the accelerometer placed on the sprung mass in the distance of tyre vertical axle, see Fig. 3. From this point of view it is necessary to rewrite the equations of motion. The vertical displacement (velocity, acceleration) of mass m_2 can be expressed as a function of geometry and displacement (velocity, acceleration) of accelerometer as follows:

$$x_2 = \left(l_2/l_1\right)\cdot x_{2a},\ \dot{x}_2 = \left(l_2/l_1\right)\cdot \dot{x}_{2a},\ \ddot{x}_2 = \left(l_2/l_1\right)\cdot \ddot{x}_{2a} \quad (25)$$

After substituting Eq. 25 into Eqs. 23 and 24 we can rewrite these relations as:

$$m_1\ddot{x}_1 + b_2\frac{a^2}{l_1^2}\left(\dot{x}_1 - \dot{x}_{2a}\right) + k_2\frac{a^2}{l_1^2}\left(x_1 - x_{2a}\right) + k_1 x_1 = k_1 x_0 \quad (26)$$

$$m_2\ddot{x}_{2a} + b_2\frac{a^2}{l_2^2}\left(\dot{x}_{2a} - \dot{x}_1\right) + k_2\frac{a^2}{l_2^2}\left(x_{2a} - x_1\right) = 0 \quad (27)$$

Following the equations (19) – (27) were calculated dynamic responses of sprung mass of JP VŠDS indicated by speed control bump – type CZ 8 – Fig.4.

The simulated responses were calculated in the algorithm IRI – KCS. The measured accelerations were obtained by transducer B 12/200 of the HBM company (intensive by circle in Fig.3) - an inductive type of a scanner of a working frequency 0 - 100 Hz and sensibility of 0 - 200 m.s^{-2}. The comparison measured and simulated accelerations can be seen in Fig.5.

Fig. 4. Measuring set JP VŠDS and speed control bump – type CZ 8

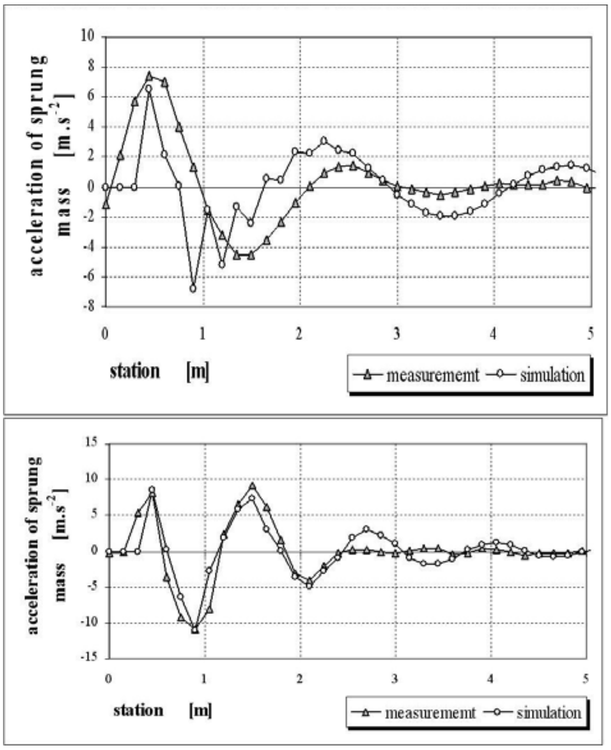

Fig. 5. Comparison of measured and simulated dynamic response of sprung mass of JP VŠDS indicated by speed control bump – type CZ 8

4. Power spectral density of longitudinal unevenness

The discretionary evaluated road sections, which are homogenous from the point of view of construction and degradation conditions, can be evaluated through the medium theory of stationary random process. This type of random process can be best characterized by a correlation function or power spectral density (PSD). The correlation function $K_h(\lambda)$ for this type of process is expressed in linear domain by equation

$$K_h(\lambda) = \int_{-\infty}^{\infty}\int_{-\infty}^{\infty}\left[h_1(l)-E_h\right]\cdot\left[h_2(l-\lambda)-E_h\right]\cdot f_2(h_1,h_2)\,dh_1\cdot dh_2 \quad (28)$$

Where: λ - linear lag [m], E_h - expected value of stochastic unevenness; $E_h = 0$, $h(l)$ - stochastic unevenness, $f_2(h_1,h_2)$ - combination density of expectation.

Stochastic unevenness is computed as a difference between a real and theoretical profile. In our case we must identify elevations of longitudinal profile per 0.25 m and longitudinal unevenness are evaluated through the standardized correlation function $\rho_h(\lambda)$ (left hand side of Fig.6).

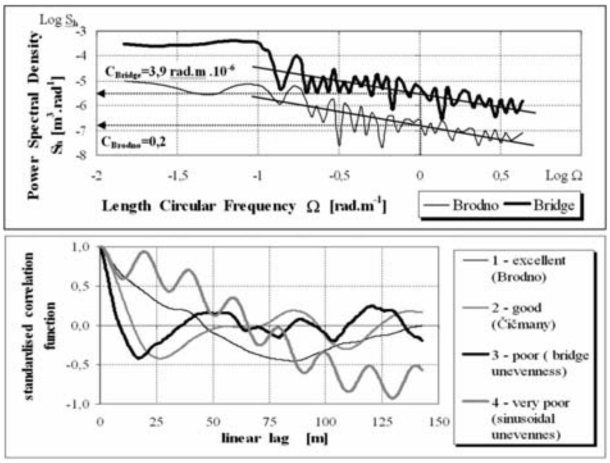

Fig. 6. Standardized correlation function and PSD of stochastic unevenness

For the purpose of unevenness assessment it is more appropriate to use power spectral density (PSD) $S_h(\mathbf{\Omega})$ (right hand side of Fig.6), which can be expressed from the correlation function by means of Wiener Chinchine equation:

$$S_h(\Omega) = 2/\pi \cdot \int_0^{\infty} K_h(\lambda)\cdot\cos(\Omega\lambda)\cdot d\lambda \quad (30)$$

Where: D_h - dispersion of an stochastic unevenness [m^2], $\mathbf{\Omega}$ - angular spatial frequency [rad.m^{-1}],

$$\Omega = 2\cdot\pi/L \quad (31)$$

L - unevenness wavelength [m].

The unevenness degree C [rad.m.10^{-6}] of an evaluated road section is expressed from the basic relation [9] that was modified for our mode of unevenness identification by JP VŠDS.

$$C = \frac{D_y}{I\cdot\frac{1}{N}\sum_{i=1}^{n} v_i} \quad (32)$$

Where: D_y - dispersion of sprung mass acceleration – left hand side of Fig.3 [m2.s-4], I - parameter of dynamic transfer [rad^{-1}.s^{-3}], C - unevenness degree – right hand side of Fig.3 [rad.m], v_i - digital values of a measured velocity – right hand side of Fig.3 [m.s-1]

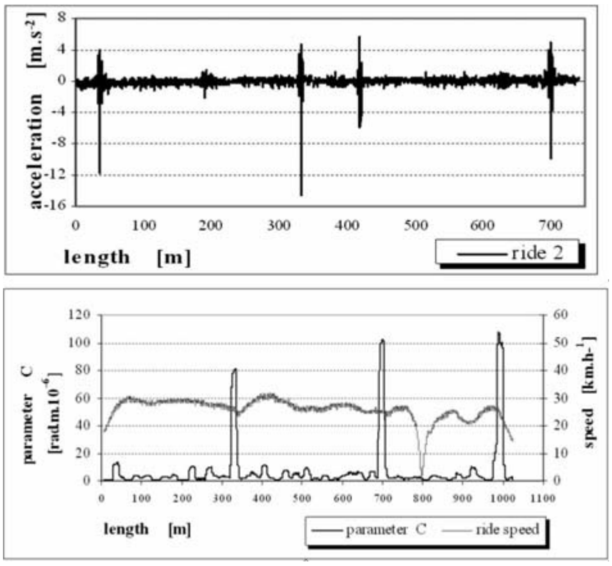

Fig. 7. Vertical acceleration indicated by speed control bump and ride speed (left hand side of Fig.7) and parameter C evaluated by JP VŠDS

4. Correlations between unevenness parameters C and IRI

The correlations between unevenness parameters *C* and *IRI* (International Roughness Index) have been determined for a consideration of theoretical dynamical response of RQCS (Reference Quarter Car Simulation) [8] and experimental measurements (Fig. 8 and 9).

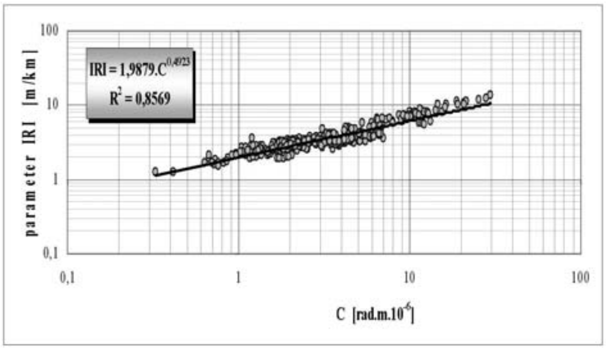

Fig. 8. Correlations of unevenness parameters C and IRIC a IRI for ride speed 90 kph

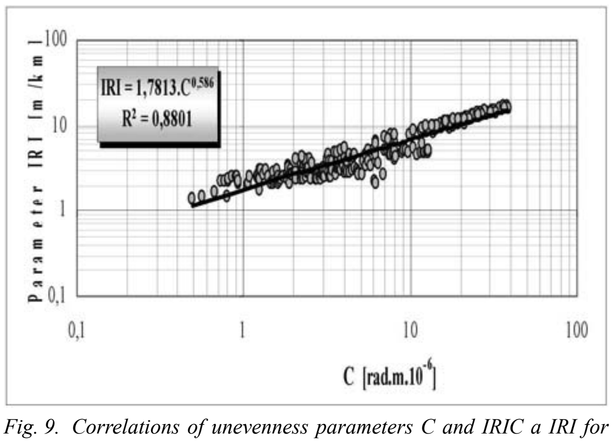

Fig. 9. Correlations of unevenness parameters C and IRIC a IRI for ride speed 130 kph

The comparison of our correlation dependences (roads - ride speed of 90 kph and highways of 130 kph) with results of the Second International PIARC-WRA experiment (including FILTER programme) [3,8] can be seen in Fig. 10.

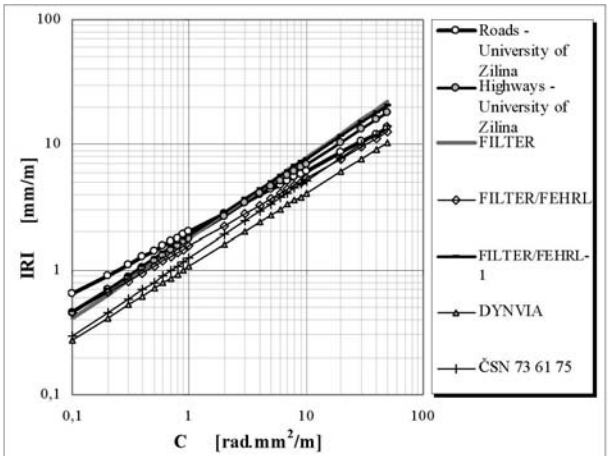

Fig. 10. Comparison of Slovak and World–wide correlation dependences between unevenness degree C and IRI

5. The criteria of unevenness evaluating by IRI

The criteria are base on described theoretical principles, and on the request of traffic safety and ride comfort assurance. The ride comfort described by vertical acceleration of sprung mass of vehicle a_z and the safety described by vertical dynamic strength F_z on the contact of the wheel with pavement surface are described in next. The simulation of the crossing of a half car model on generated harmonized unevenness as a random unevenness on real roads, measured by Profilograph GE, were realized for determination of the relation between longitudinal unevenness and ride comfort (safety, respectively). The values of maximal acceleration of the vehicle body characterizing ride discomfort occasioned by unevenness were compared according to Slovak standard STN ISO 2631-1.

The calculations and simulations were executed by using of the special software developed in University of Zilina [1] and with the CarSim Education program developed in University of Michigan [9]. The vehicle parameters correspond to Skoda Felicia car what is widespread in Slovakia.

The response depended on amplitude and wavelength by three ride speeds were detected for harmonized unevenness generated by simulation and described by IRI. Three maximal speeds permitted on the Slovak roads were used. The results for speed 90 kph will describe. From Fig.11 is definite, which wavelength activated maximal oscillation of the vehicle.

There are the wavelengths that are the most unfavourable for passenger comfort. For declared vehicle and speed 90 kph, it is 2.3 m and 18 m. For 60 kph speed, it is 2.1 m and 12 m and for 130 kph speed 3.3 m and 27 m. The model response on harmonize unevenness is linearly depending on amplitude value. The relation between vehicle response and IRI was evaluated in next. The relation between acceleration a_z and IRI, corresponding presented wavelengths with amplitude A=1 cm and speed 90 kph are showed in Fig. 12.

Following to analyze we can claim the values of the vehicle body acceleration increases with growing of IRI only to

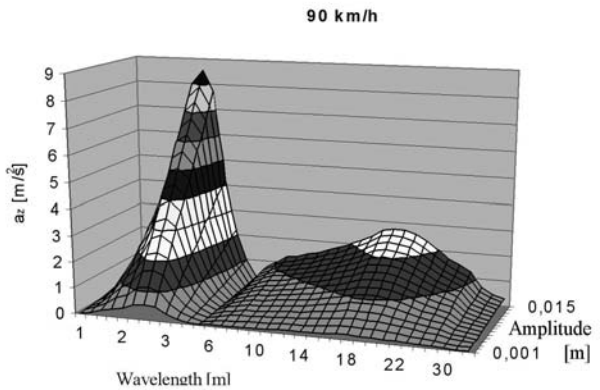

Fig. 11. The dependency between acceleration, wavelengths and amplitudes for 90 kph speed

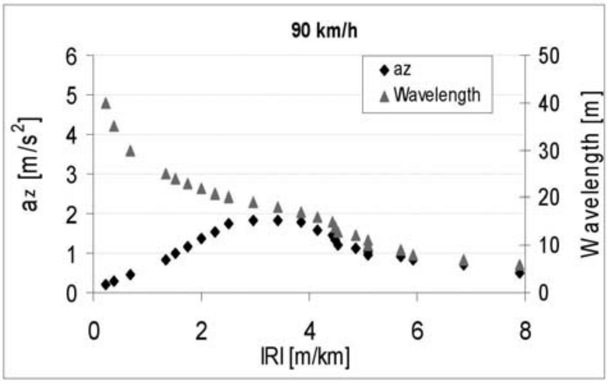

Fig. 12. The dependency between acceleration, wavelength, and IRI for 90 km/h speed

specific point. This point corresponds to specific wavelengths depended on the speed. Decreasing tendency despite of IRI growing was observed after this point. On the Fig. 7 are these relations extensive about next points, which responsive higher amplitudes. The relation tendency shows a basic trend of points that delimited an area of maximal discomfort by minimal IRI values. The line by basic points group was interleaved for determination of the relation between IRI and a_z. The other points lying below tendency are irrelevant from comfort evaluation point of view. The upper values of IRI respond the lower values of the response. The points above this group (by speed 60 kph) respond the great wavelengths (more than 30 m), which do not exist on the roads with maximal speed 60 kph. Therefore, we can ignore them.

The Fig. 13 shows determined relation between IRI and vehicle response characterized by vertical acceleration a_z, found from a fitted line equation of basic tendency of the points.

The points out of basic tendency confirm that equal value of IRI can describes more unevenness evocated different response. These points have identical amplitude but different wavelength, what means lower value of acceleration for higher IRI. The visible is also that during high speeds a shining oscillation of the vehicle origins for low IRI value. This fact is determined by overvaluation of the short wavelengths and undervaluation the longer wavelengths by reference model of a car quarter. In addition, IRI is calculated for speed 80 kph so for higher speed the differences are more (Fig. 14). However, we must take into consideration that the simulation was realized for harmonic unevenness that occur in real condition in minimal range.

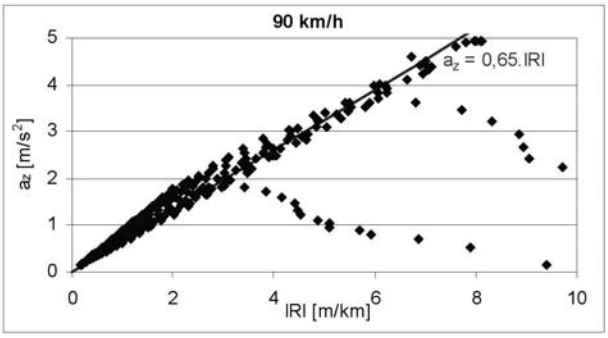

Fig. 13. The relation of acceleration on IRI for 90 kph

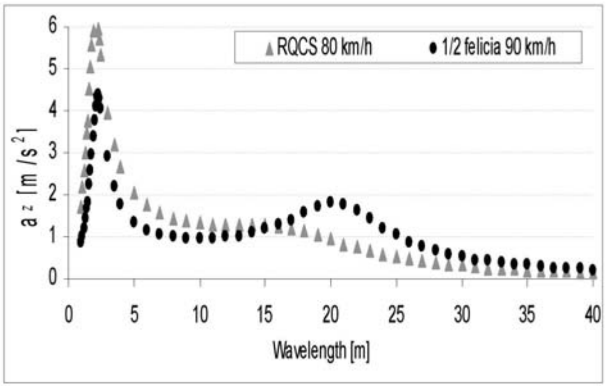

Fig. 14. The comparison of response for different speeds of reference and real model

According to obtained relations, the scale of IRI evaluation depends on safety and comfortable was analyzed. The results show that critical rank of evaluation of real response to unevenness is wavelengths corresponding with resonant frequency of car unsprung mass. The reference model declares lower values of acceleration of the sprung mass as real car model. The values are two times more for speed 90 kph and four times more for speed 130 kph. Depend on analysis of the harmonic unevenness, the simulations realized on the real road sections was taking into account for design of IRI classification scale.

The important characteristic of ride safety from point of view of longitudinal unevenness is the vertical strength F_z on the contact between vehicle and surface. The moment of minimal value was observed. The determined relation is presented on Fig. 15.

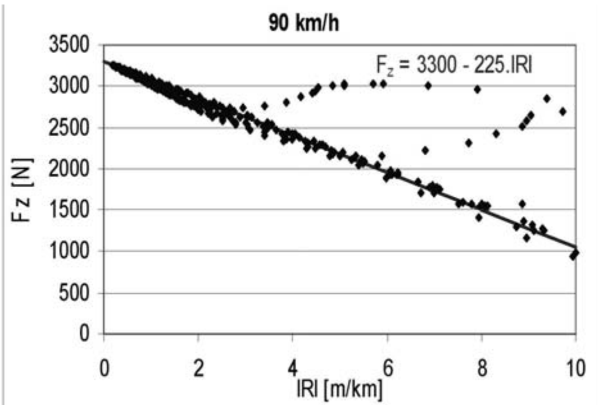

Fig. 15. The dependency of dynamic strength F_z on IRI for speed 90 km/h

The strength F_z has decreasing tendency with increasing of IRI. The different values of F_z for identical IRI value are possible to achieve alike for acceleration. During simulation of harmonic unevenness and speed 60 kph the loss of contact does not occur. On the other hand, during speed 90 kph and 130 kph the F_z achieved the zero value yet for low IRI values. The danger is not only a loss of contact but a low intensity of F_z, too. An intensity of the vertical strength has influence to the stability of a car in horizontal curve and to the breaking distance, too. The differences are determined by characteristics of the reference model. In this case, the generally valid relation is not possible to establish because each vehicle has different weight so also different press strength of axle to the road surface. Depend on presented results the new classification scale for IRI evaluation in frame of Slovak PMS was proposed (Table 1).

Tab.1 The proposal of classification scale of IRI

Classification scale	*IRI [m/km]*		
	Urban roads	*Roads*	*Highways and expressways*
1	*< 5*	*< 4*	*< 3*
2	*5 - 10*	*4 - 8*	*3 – 6*
3	*> 10*	*> 8*	*> 6*

6. Conclusions

Presented results are based on the data sample that contents the real conditions. The research activity on problems of the interaction between vehicle and surface continues. The analyses of unevenness and skid resistance are in process for results improving. The verification of the models is verified by next measurements and simulations. The aim of the research is generalization of relation between IRI and vehicle response.

7. Preferences

[1] Celko, J. et al: *Surface properties of the pavements (in Slovak),* Scientific monograph. EDIS Zilina, 2000, ISBN 80-7100-774-9.

[2] Kropac, O., Mucka, P.: *Be careful when using the International Roughness Index as an indicator of road unevenness.* Journal of Sound and Vibration, Vol. 287, 2005, Nos. 4-5, ISSN: 0022-460X, pp. 989-1003.

[3] Kropac, O., Mucka, P.: *Relations between characteristics of longitudinal unevenness of roads: a review,* Strojnicky casopis, 1/2003, ISSN 0039-2472, pp.49-64.

[4] Kropac, O., Sprinc, J., Sprinc, M.: *Using of results of international harmonisation experiment EVEN – FILTER: longitudinal unevenness of pavements (in Czech),* Silnicni obzor, 2/2003, ISSN 0322-7154, pp. 37-48.

[5] Sayers, M. W., Gillespie, T. D., Queiroz, C.: *The International Road Roughness Experiment (IRRE): Establishing correlation and calibration standard for easurements,* World Bank, Techn. Paper, No. 45.

[6] Sun L.: *Developing spectrum-based models for International Roughness Index and Present Serviceability Index.* In: ASCE: Journal of Transportation EngineeringVol. 127, No. 6, 2001, ISSN: 0733-947X p. 463-470.

[7] TP 10/2006 *Pavement Management System (in Slovak), Technical regulation,* MTPT SR, 2006.

[8] World Road Association: *International experiment to harmonize longitudinal and transverse profile measurement and reporting procedure,* PIARC technical Committee on Surface Characteristics, 2002.

[9] Tutorial for CarSim Educational: An 18 – DOF Vehicle Dynamics Simulation, Mechanical Simulation Corporation, Michigan, www.trucksim.com.

****

The article was preparing with the support of Slovak Grant Agency VEGA – project 1/3339/

****

Prof. Ing. Jan CELKO CSc.
Doc. Dr. Ing. Martin DECKÝ
Ing. Matúš KOVÁČ, Ph.D.

Faculty of Civil Engineering, Highway Engineering Department.
Komenskeho 52, 010 26 Zilina, Slovakia
tel: +421 41 7232145
e-mail: jan.celko@fstav.uniza.sk, decky@fstav.uniza.sk, kovac@fstav.uniza.sk